



# The effect of bulk concentration gradient on fluid–solid reaction rate

Manuel Perez-Tello<sup>a</sup>, Hong Yong Sohn<sup>a,b,\*</sup>, Raj K. Rajamani<sup>b</sup>

<sup>a</sup>Department of Chemical and Fuels Engineering, University of Utah, 135 S. 1460E. Rm 412, Salt Lake City, Utah 84112-0114, USA

<sup>b</sup>Department of Metallurgical Engineering, University of Utah, 135 S. 1460E. Rm 412, Salt Lake City, Utah 84112-0114, USA

Received 10 December 1997; accepted 13 August 1998

## Abstract

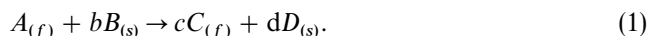
Considerable attention has been paid to the development of mathematical models to describe fluid–solid reaction systems as they play a significant role in many chemical, metallurgical, and other engineering areas. The present work is aimed at examining one of the assumptions generally made in the mathematical modeling of fluid–solid reaction systems; namely, that the bulk concentration of the fluid reactant is uniform around the solid surface. This is a reasonable assumption under well-mixed conditions of the fluid phase. However, under certain conditions, concentration gradients in the axial direction in the fluid near the surface may be present; a packed bed is an example of such a case. It is of interest to investigate how large the concentration gradient should be before the assumption of a uniform bulk concentration around a pellet to cause a significant error.

The effect of a fluid concentration gradient has been studied for a catalytic reaction on the external surface of a nonporous sphere. Petersen et al. (1964) found that external concentration gradients do not significantly affect the overall reaction rate except for the case of a second-order reaction when the reactant concentration drops from its maximum value to zero over the distance of a particle diameter, which is a rather unlikely situation in practice. Similar results were obtained by Acrivos and Chambré (1957), who recommended the use of this approximation with caution when a series of consecutive reactions takes place. In many fluid–solid reactions, the reaction progresses towards the interior of the pellet as the solid reactant near the external surface is consumed, leaving behind either a porous solid product or inert solid matrix. Although it is generally believed that a bulk concentration gradient does not significantly affect the behavior of most noncatalytic fluid–solid reactions of industrial relevance, no formal verification of this statement has yet been provided in the literature. In this work, the validity of this hypothesis is tested for a simple fluid–solid reaction configuration. © 1999 Elsevier Science Ltd. All rights reserved.

**Keywords:** Concentration gradient; Fluid–solid reaction; Grain model; Monte Carlo simulation; Random walk

## 1. Problem formulation and numerical solution

Fig. 1 shows a schematic representation of the system considered in this study. The grain model reported by Sohn and Szekely (1972) is followed here to represent the solid phase, where a spherical pellet made up of initially nonporous grains each undergoing a topochemical reaction is shown as an example. The following fluid–solid reaction is assumed to occur:



The assumptions made in the grain model were reported by Sohn and Szekely (1972). The validity and applica-

bility of these assumptions in many practical reaction systems have been well documented (Sohn and Szekely, 1972; Szekely et al., 1973; Szekely et al., 1976), and thus are not repeated here. The grain model equations can be written as

$$\nabla^2 \psi - 2F_g F_p \sigma^2 \zeta^{F_g - 1} \psi = 0, \quad (2)$$

$$\frac{\partial \zeta}{\partial t^*} = -\psi, \quad (3)$$

where

$$\psi = C_A / \bar{C}_{A,s}, \quad (4)$$

$$\zeta = \frac{A_g r_c}{F_g V_g}, \quad (5)$$

\*Corresponding author. Tel.: 001 801 581 5491; fax: 001 801 581 4937; e-mail: hysohn@mines.utah.edu.

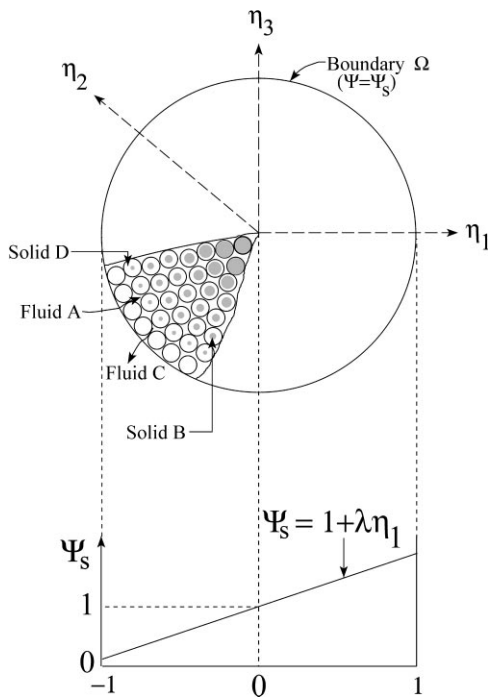


Fig. 1. Schematic representation of a spherical pellet made up of grains in the presence of a linear bulk concentration gradient of reactant fluid A.

$$\hat{\sigma} = \frac{V_p}{A_p} \sqrt{\frac{(1-\varepsilon)kF_p}{2D_e} \left(\frac{A_g}{F_g V_g}\right)}, \quad (6)$$

$$t^* = \frac{bk}{\rho_s} \left(\frac{A_g}{F_g V_g}\right) \bar{C}_{A,s} t. \quad (7)$$

The Laplacian operator in Eq. (2) is defined in Cartesian coordinates with respect to the normalized quantities  $\eta_1 = xA_p/F_pV_p$ ,  $\eta_2 = yA_p/F_pV_p$ , and  $\eta_3 = zA_p/F_pV_p$ . Eqs. (2) and (3) describe the dimensionless concentration of reactant A in the pellet and the dimensionless position of the reaction interface in the grain, respectively, as functions of time and position within the pellet. Eqs. (2) and (3) were solved subject to the boundary conditions:

$$\text{B.C.1: at } t^* = 0, \xi = 1 \quad \text{for all } \eta_1, \eta_2, \eta_3 \in \Omega, \quad (8)$$

$$\text{B.C.2: } \psi = \psi_s = 1 + \lambda\eta_1 \quad \text{at the pellet surface.} \quad (9)$$

In B.C.2, the bulk concentration has been assumed to vary linearly along the  $\eta_1$ -axis and the external diffusion resistance has been neglected; the slope of the straight line  $\psi_s$  vs  $\eta_1$  is the dimensionless concentration gradient  $\lambda$  (Fig. 1). It is noted that  $\lambda$  can only take on values between 0 and 1, since  $\psi_s$  is set to unity at  $\eta_1 = 0$  ( $\eta_2, \eta_3$  at the surface) and  $\psi_s$  cannot be negative. The linear relationship in Eq. (9) insures that the average dimensionless bulk concentration of fluid A is equal to unity in all cases. This choice is deliberate in order to compare the results obtained for an arbitrary  $\lambda$  value with the results from the uniform concentration case:  $\lambda = 0$ ,  $\psi_s = 1$ ; the extreme

case is  $\lambda = 1$  for which  $\psi_s$  drops from a maximum value of 2 to zero over the distance of a pellet diameter. For the spherical pellet considered,  $F_p = 3$ , and the pellet surface is defined by the geometric relationship:  $\eta_1^2 + \eta_2^2 + \eta_3^2 = 1$ .

Eqs. (2) and (3) subject to Eqs. (8) and (9) can be solved by specifying three parameters:  $F_g$ ,  $\hat{\sigma}$ , and  $\lambda$ .  $F_g$  represents the grain geometry with values of 1, 2, and 3 for infinite slabs, long cylinders, and spheres, respectively;  $\hat{\sigma}$  is the generalized reaction modulus whose value varies from zero (reaction control) to infinity (diffusion control).

The numerical solution of Eqs. (2) and (3) was based on the algorithm developed by Rajamani (1989). Eq. (2) was cast into finite-difference equations and solved by a Monte Carlo method using a series of random walks throughout the interior of the pellet and ending at the surface. Eq. (3) was solved simultaneously at each grid-point using a third-order Runge–Kutta method. The fractional conversion of the solid pellet at time  $t^*$  was computed from the following expression:

$$X = \frac{\int_{\eta_1} \int_{\eta_2} \int_{\eta_3} (1 - \xi^{F_g}) d\eta_1 d\eta_2 d\eta_3}{\int_{\eta_1} \int_{\eta_2} \int_{\eta_3} d\eta_1 d\eta_2 d\eta_3} \quad (10)$$

for which a 3D-Simpson's numerical integration technique was used.

## 2. Results and discussion

The conversion vs time results for different values of  $\hat{\sigma}$  and  $\lambda$  are shown in Fig. 2a and b when the grains consist of infinite flat slabs ( $F_g = 1$ ). For other grain geometries (i.e.,  $F_g = 2, 3$ ) the results were similar to those shown in these figures and thus not shown here. It is noted that according to the criteria developed by Sohn (1978) and Sohn and Szekely (1972), the case  $\hat{\sigma} = 0.1$  and 10 represent, respectively, essentially (within 1%) rate control by chemical reaction and pore diffusion.

The case  $\lambda = 0.5$  is a case in which the concentration of the fluid reactant reduces down to one-third its maximum concentration over the distance of a particle diameter. It is seen that this concentration gradient has no substantial effect on the reaction rate up to 80% conversion for all  $\hat{\sigma}$ , but the times for higher conversion values are significantly affected for the case of a small  $\hat{\sigma}$ . In fact, for  $\hat{\sigma} = 0$  (no pore-diffusion effects) the time for complete conversion would in this case be twice that for the case of  $\lambda = 0$ .

The case  $\lambda = 1$  is unrealistic in practice but represents the extreme situation. Here, the concentration of the fluid reactant reduces down to zero from its maximum value over the distance of a particle diameter. In this case the deviation from the case of a uniform concentration becomes significant at conversion values greater than 60%, the effect becoming larger as  $\hat{\sigma}$  becomes smaller. It is also

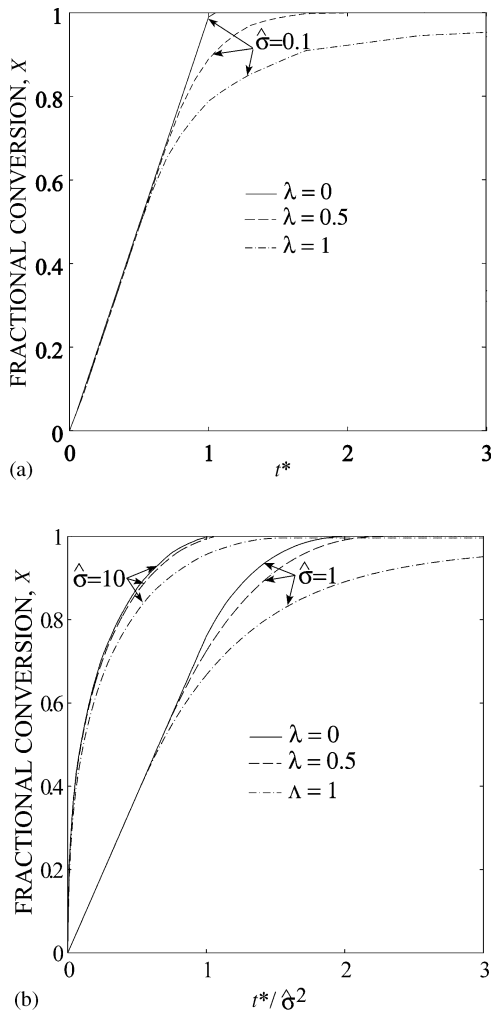


Fig. 2. Conversion vs time plots for a spherical pellet made up of flat-slab grains for different values of  $\lambda$ . (a)  $\hat{\sigma} = 0.1$ ; (b)  $\hat{\sigma} = 1$  and 10.

noted that the time for complete conversion in this case is infinity for any  $\hat{\sigma}$ . This is because the fluid concentration at  $\eta_1 = -1$  is zero, and the solid at this location will undergo no reaction.

The effect of concentration gradient on noncatalytic fluid–solid reactions is quite different from that on catalytic reactions, either on the surface of a nonporous sphere or in a porous pellet. In catalytic reactions in which the solid remains unchanged, if diffusion is fast and the reaction is of first order, the overall rate does not change with concentration gradient as long as the average concentration remains the same. In the former, the solid is consumed and thus the bulk-concentration gradient affects the reaction even if it is of first order with respect to the fluid-reactant concentration. Most obviously, the time for complete conversion of the solid is determined by the lowest value of the fluid–reactant concentration. This explains the overall trends observed in Fig. 2. A practical situation where a large concentration gradient across the pellet might exist would be a shal-

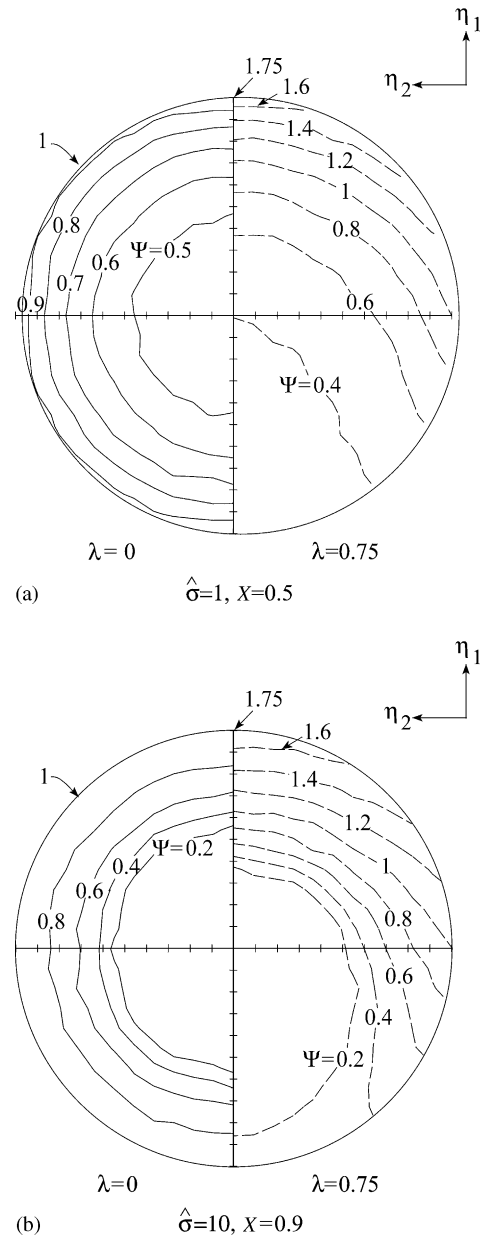


Fig. 3. Concentration contours of the reactant fluid A within a spherical pellet made up of flat-slab grains for different values of  $\lambda$ . (a) 50% solid conversion and  $\hat{\sigma} = 1$ ; (b) 90% solid conversion and  $\hat{\sigma} = 10$ .

low packed bed in which the fluid reactant is almost completely consumed across the layer of the packed solid.

The effect of a concentration gradient is expected to be smaller for reactions of orders lower than one, which is the case for some fluid–solid reactions. On the other hand, a temperature gradient across a solid pellet could have a stronger effect because of the exponential dependence of the chemical kinetics on temperature.

To test the effect of a concentration gradient on the shape of the concentration contours of the fluid reactant within the solid pellet, the case  $\lambda = 0.75$  was simulated.

The results obtained are shown in Fig. 3. At 50% solid conversion and  $\hat{\sigma} = 1$  (Fig. 3a) the concentration contours change from concentric to skewed as  $\lambda$  increases from zero to 0.75. For  $\hat{\sigma} = 1$ , chemical kinetics and intrapellet diffusion are of similar importance, and thus the concentration contours span over the entire pellet volume. At 90% solid conversion and  $\hat{\sigma} = 10$  (Fig. 3b) the concentration contours at  $\lambda = 0.75$  are also skewed but are now confined to a reaction zone surrounding a core of unreacted solid. This is because at  $\hat{\sigma} = 10$  the system approaches the diffusion control regime, and the reaction front progresses in a similar way to the shrinking-core scheme.

The results discussed in this work indicate that for most practical applications, a bulk concentration gradient would not significantly affect the rate of a noncatalytic fluid–solid reaction. The effect of a concentration gradient, however, becomes significant at high values of the fractional conversion, especially when the system approaches the reaction control regime. In practice, this situation would correspond to a shallow packed bed in which the fluid reactant is almost completely consumed. The effect is expected to be smaller for reactions of lower orders.

### Acknowledgements

MPT expresses his gratitude to CONACYT, Universidad de Sonora (Mexico) and the IIE-Fulbright Program (USA) for providing his scholarship grants during this work.

### Notation

|              |   |
|--------------|---|
| $A$          | surface area, $\text{m}^2$  |
| $C, \bar{C}$ | concentration, average concentration, $\text{mol}/\text{m}^3$                           |
| $D_e$        | effective diffusivity of $A$ in the porous pellet, $\text{m}^2/\text{s}$                |
| $F_p$        | shape factor (= 1, 2, and 3 for flat slabs, long cylinders, and spheres, respectively). |
| $k$          | reaction-rate constant, $\text{m}/\text{s}$   |
| $r_c$        | position of moving reaction front in the individual grain, $\text{m}$                   |
| $t^*$        | dimensionless time defined by Eq. (7)   |
| $V$          | volume, $\text{m}^3$  |
| $x, y, z$    | Cartesian coordinates, $\text{m}$   |

$X$  fractional conversion of pellet defined by Eq. (10)

### Greek letters

|                          |  |
|--------------------------|--|
| $\varepsilon$            | pellet porosity  |
| $\eta_1, \eta_2, \eta_3$ | dimensionless Cartesian coordinates ( $\eta_1 = xA_p/F_pV_p$ , $\eta_2 = yA_p/F_pV_p$ , $\eta_3 = zA_p/F_pV_p$ ) |
| $\lambda$                | dimensionless concentration gradient defined in Eq. (9)  |
| $\xi$                    | dimensionless position of the reaction interface in the grain defined by Eq. (5)                                 |
| $\rho_s$                 | molar density of solid grains, $\text{mol}/\text{m}^3$   |
| $\hat{\sigma}$           | Generalized fluid–solid reaction modulus defined by Eq. (6)  |
| $\psi$                   | dimensionless concentration of reactant A within the pellet defined by Eq. (4)                                   |
| $\psi_s$                 | dimensionless concentration of reactant A on the pellet surface  |
| $\Omega$                 | pellet boundary  |

### Subscripts

|     |         |
|-----|---------|
| $f$ | fluid   |
| $g$ | grain   |
| $p$ | pellet  |
| $s$ | surface |

### References

- Acrivos, A., & Chambré, P.L. (1957). Laminar boundary layer flows with surface reactions. *Ind. Engng. Chem.*, 49, 1025–1029.
- Petersen, E.E., Friedly, J.C., & DeVogelaere, R.J. (1964). The rate of chemical reaction at the surface of a non-porous catalytic sphere in concentration and temperature gradients-I. Steady state solutions. *Chem. Engng Sci.*, 19, 683–692.
- Rajamani, K. (1989). Reaction of an irregular particle with a gas: Monte Carlo method for the solution of the pellet–grain model. *Chem. Engng Sci.*, 44, 2345–2353.
- Sohn, H.Y. (1978). The law of additive reaction times in fluid–solid reactions. *Metall. Trans.*, B 9B, 89–96.
- Sohn, H.Y., & Szekeley, J. (1972). A structural model for gas–solid reactions with a moving boundary-III. A general dimensionless representation of the irreversible reaction between a porous solid and a reactant gas. *Chem. Engng Sci.*, 27, 763–778.
- Szekeley, J., Lin, C.L., & Sohn, H.Y. (1973). A structural model for gas–solid reactions with a moving boundary-V. An experimental study of the reduction of porous nickel-oxide pellets with hydrogen. *Chem. Engng Sci.*, 28, 1975–1989.
- Szekeley, J., Evans, J.W., & Sohn, H.Y. (1976) *Gas–solid reactions*. (pp. 125–161). New York: Academic Press.